RESEARCH ARTICLE

ScienceAsia 30 (2004): **399-410**

Adsorption of Palladium on MgO/Al_2O_3 and CuO/Al_2O_3

Supaporn Therdthianwong* Ampon Tongsima and Apichai Therdthianwong

Chemical Engineering Practice School, Faculty of Engineering, King Mongkut's University of Technology Thonburi, 91 Pracha Utis Rd., Bangmod, Tungkru, Bangkok 10140 Thailand.

* Corresponding author: E-mail: supaporn.the@kmutt.ac.th

Received *25 Mar 2004*
Accepted *11 Aug 2004*

ABSTRACT: An adsorption model explaining and predicting the adsorption phenomena of palladium complex ions over MgO/Al_2O_3 and CuO/Al_2O_3 was developed based on the triple layer theory. Wet impregnation or adsorption experiments were conducted to determine the solution variables and some parameters used in the model and to verify the adsorption model. Adsorption of palladium complex ions on pure oxides (Al_2O_3, MgO and CuO) and composite oxides (3% and 15% of MgO and CuO on Al_2O_3) was investigated at different solution pH. From the experiments, Pd adsorption capability of pure and composite oxides was influenced by solution pH, type of promoter on the support and concentration of promoter. Overall the results predicted from the triple layer model agreed reasonably well with the experimental data, except in the pH range near the point of zero charge of oxide. The suggested pH value for preparing $Pd/MgO/Al_2O_3$ and $Pd/CuO/Al_2O_3$ composite oxides is the pH close to the initial pH of the palladium precursor solution.

KEYWORDS: triple layer model, Pd adsorption, MgO/Al_2O_3, CuO/Al_2O_3

INTRODUCTION

The ion exchange of metal ions and their complexes on oxide supports plays an important role in various applications, for example, purification processes, integrated circuit fabrication, and catalyst preparation. For catalyst preparation, the supported metal oxide catalysts are prepared by wet impregnation that is performed by doping the porous oxide with an excess of liquid containing precursor ions of an active noble metal. This process results in a relatively high loading and high-dispersed state of the active noble metal component and its adsorption capability depends on many parameters, such as pH of solution, solid oxide loading, ionic strength etc. To deal with these factors in determining the suitable conditions for catalyst preparation, numerous experiments have to be performed. The number of experiments can be reduced by developing a mathematical model for this preparation method. Various models have been proposed to explain the adsorption phenomena of metal ions on oxide supports, describing the surface charge development on oxides, and predicting the effect of such parameters in the catalyst preparation. One of the most suitable and applicable adsorption models used is the "triple layer model" (TLM).

The triple layer model was first developed from the electrical double layer model by Yates and Healy[1] and further modified by Davis et al[2] to study behavior of oxide/electrolyte interfaces. It can explain the adsorption of ions in aqueous solution on solid surfaces phenomenon, since its nature is more chemical than physical. The model proved to be applicable for various adsorption systems [3,4,5,6].

Modeling of noble metal complex ions adsorbed onto single oxides has been given more attention than composite oxides, although the latter are used in many industries. TLM, though apparently suitable for explaining adsorption in the oxide-liquid system, has not yet been applied to composite oxides. MgO/Al_2O_3 and CuO/Al_2O_3, common catalyst supports widely used in hydration-dehydration reactions, were chosen to study in this work in order to understand how the two oxides influence the adsorption capability of palladium complex ions on alumina.

Theory and Adsorption Modeling

The system in the adsorption model is divided into three regions: oxide surface region, oxide-liquid interface region and bulk liquid region, as shown in Fig. 1. The TLM concept is applied in the former two regions. Equations in the adsorption model are described below.

i) Oxide Surface Region (Region I) [7]

In this region, the charge is involved in the adsorption and desorption of protons and background electrolytes.

a) Charge by Adsorption and Desorption of Protons

The charging mechanisms of an amphoteric surface caused by both adsorption and desorption of protons on the surface (S) are represented as

$$SOH_2^+ \rightleftharpoons SOH + H^+ \qquad (1)$$

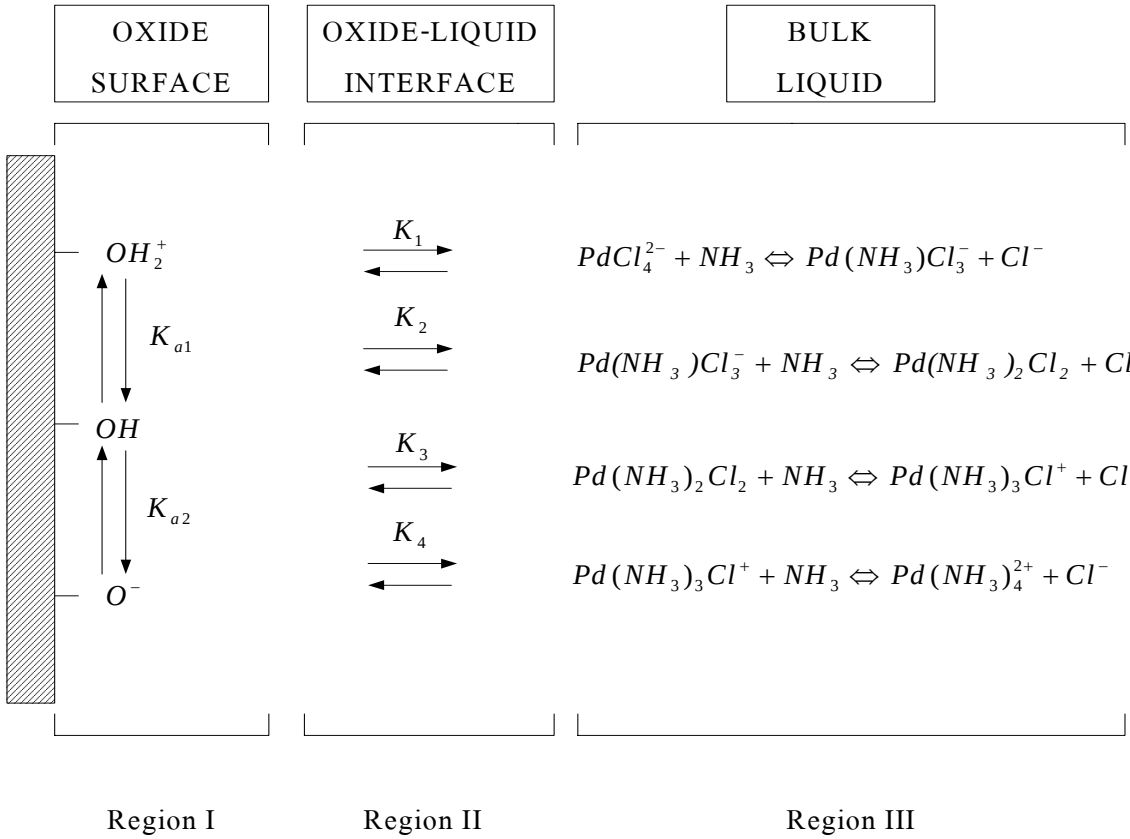

Fig 1. Schematic of adsorption/wet impregnation of Al_2O_3 with a solution of palladium chloride

$$SOH \rightleftharpoons SO^- + H^+ \qquad (2)$$

The intrinsic conditional equilibrium constants, and $K_{a_2}^{int}$, measured the tendency of the hydroxyl functional groups to undergo the above reactions can be presented as follows:

$$K_{a_2}^{int} = \frac{[SOH]\{H^+\}}{[SOH_2^+]} \exp(-e\psi_0/kT) \qquad (3)$$

and

$$K_{a_2}^{int} = \frac{[SO^-]\{H^+\}}{[SOH]} \exp(-e\psi_0/kT) \qquad (4)$$

The surface charge density (σ_0) and surface potential (ψ_0) are related by the Gouy-Chapman theory of diffuse layer as

$$\sigma_0 = 11.74\, I^{0.5} \sinh\left(\frac{ze\psi_0}{2kT}\right) \qquad (5)$$

The surface charge density is related to the surface charge concentration as:

$$\sigma_0 = \frac{10^6 F}{A}([SOH_2^+] - [SO^-]) \qquad (6)$$

b.) Charge by Complexation of Background Electrolyte

In addition to the adsorption and desorption mechanisms, partial complexation of background electrolytes may also contribute to the surface charge as follows:

$$SOH + X^+ \rightleftharpoons SO^-X^+ + H^+ \qquad (7)$$

$$SOH + H^+ + Y^- \rightleftharpoons SOH_2^+Y^- \qquad (8)$$

The intrinsic ionization constant of background electrolytes for cation, K_x^{int} and anion, K_y^{int} can be found as follows :

$$K_x^{int} = \frac{[SO^-X^+]\{H^+\}}{[SOH]\{X^+\}} \exp(-e(\psi_0 - \psi_\beta)/kT) \qquad (9)$$

$$K_y^{int} = \frac{[SOH_2^+Y^-]}{[SOH]\{H^+\}\{Y^-\}} \exp(-e(\psi_0 - \psi_\beta)/kT) \qquad (10)$$

Due to surface ionization and complexation from background electrolyte, the charge and potential at the d plane, σ_d and Ψ_d, are related by the Gouy-Chapman relation as

$$\sigma_d = -11.74 I^{0.5} \sinh\left(\frac{ze\psi_d}{2kT}\right) \qquad (11)$$

The electroneutrality requirement in the triple layer is

$$\sigma_o + \sigma_\beta + \sigma_d = 0 \qquad (12)$$

The complex electrolyte ions X^+ and Y^- are considered to situate at the β plane. Thus, the expression of the surface charge including the surface species for this case is

$$\sigma_o = \frac{10^6 F}{A}([SOH_2^+ + [SOH_2^+Y^-] - [SO^-] - [SO^-X^+]) \qquad (13)$$

The charge at the β plane, σ_β, is

$$\sigma_\beta = \frac{10^6 F}{A}([SO^-X^+] - [SOH_2^+Y^-]) \qquad (14)$$

The charge at the d plane, σ_d, can be found from the previous two equations and the electroneutrality requirement to obtain

$$\sigma_d = \frac{10^6 F}{A}([SO^-] - [SOH_2^+]) \qquad (15)$$

The expressions for the integral capacities of the inner region of the two parts are shown as

$$C_1 = \frac{\sigma_0}{\psi_0 - \psi_\beta} \qquad (16)$$

$$C_2 = -\frac{\sigma_d}{\psi_\beta - \psi_d} \qquad (17)$$

The total site density, N_s, including cationic and anionic surface charges due to adsorption/desorption of protons and electrolytes is

$$N_s = \frac{N_A}{A}([SOH] + [SOH_2^+] + [SO^-] + [SOH_2^+Y^-] + [SO^-X^+]) \qquad (18)$$

Equations (3), (4), (9) through (11), and (13) through (18) constitute the system of equations describing surface charging due to adsorption and desorption of hydrogen in combination with electrolyte complexation and the use of the triple-layer model for the electrical double layer. Among these 11 equations, 21 variables and parameters are present: σ_o, σ_β, σ_d, ψ_o, ψ_β, ψ_d, C_1, C_2, N_s, K_x^{int}, K_y^{int}, $K_{a_1}^{int}$, $K_{a_2}^{int}$, $\{H^+\}$, $\{X^+\}$, $\{Y^-\}$, $[SO^-X^+]$, $[SOH_2^+Y^-]$, $[SOH]$, $[SO^-]$, and $[SOH_2^+]$. Thus, if the system and solution variables and parameters are specified, namely, values of C_1, C_2, N_s, K_x^{int}, K_y^{int}, $K_{a_1}^{int}$, $K_{a_2}^{int}$, $\{H^+\}$, $\{X^+\}$, and $\{Y^-\}$, then the 11 variables can be readily determined from the 11 equations.

The value of C_1 typically used was around 100-140 $\mu F / cm^2$ whereas the value of C_2 was kept constant at 20 $\mu F/cm^2$ which is the magnitude of capacitance at Hg/H_2O and AgI/H_2O interfaces [8].

The values of $K_{a_1}^{int}$ and $K_{a_2}^{int}$ were determined from the pH_{pzc} (measured in the experiment) together with the DpK value, the difference between two pK^{int} values obtained from a similar system in the work of Schwarz et al [9] and Davis et al [2] defined as follows:

$$pH_{pzc} = \frac{(pK_{a_1}^{int} + pK_{a_2}^{int})}{2} \qquad (19)$$

$$DpK = pK_{a2}^{int} - pK_{a1}^{int} \qquad (20)$$

DpK is an important parameter for determining the pH-dependent distribution of ionizable surface groups.

In case of the intrinsic equilibrium constants of background cationic and anionic electrolytes, K_x^{int} and K_y^{int}, the difference of these values was chosen and obtained from a similar system in the literature [5].

$$DpX = pK_x^{int} - pK_y^{int} \qquad (21)$$

The value of N_s in the case of pure Al_2O_3, about 1×10^{15} sites/cm^2, was obtained from the literature[8]. The values of N_s in the case of other pure oxides (CuO and Al_2O_3) and composite oxides were estimated based on the BET surface area of each oxide compared with Al_2O_3. Solution variables, such as $\{H^+\}$, $\{X^+\}$ and $\{Y^-\}$, can be readily determined from the adsorption experiments.

ii) Liquid-Oxide Interface Region (Region II) [10]

The amount of Pd adsorbed on an oxide surface can be determined from this region. This region is the combination between oxide surface region (region I) and liquid bulk region (region III). The amount of Pd species adsorbed in terms of adsorption density is represented by Grahame's equation [10] as

$$\Gamma_i = 2r_{hydrated} C_i \exp(-\Delta G^{o}_{ads,i}/RT) \quad (22)$$

For adsorption of hydrolyzable metal ions, the free energy of adsorption, $\Delta G^{o}_{ads,i}$ is classified into three terms: coulombic, solvation, and chemical free energy [11] :

$$\Delta G^{o}_{ads,i} = \Delta G^{o}_{coul,i} + \Delta G^{o}_{solv,i} + \Delta G^{o}_{chem,i} \quad (23)$$

The coulombic contribution of species 'i', $\Delta G^{o}_{coul,i}$, is given as

$$\Delta G^{o}_{coul,i} = z_i F \psi_{x,i} \quad (24)$$

where $\psi_{x,i}$ is the solution of the Laplace's equation subject to the surface and bulk boundary conditions obtained from the Gouy and Chapman electric double layer model and is in the form of

$$\psi_{x,i} = \frac{2RT}{F} \ln\left[\frac{\{\exp(zF\psi_0/2RT)+1\} + \{\exp(zF\psi_0/2RT)-1\}\exp(-\kappa x_i)}{\{\exp(zF\psi_0/2RT)+1\} - \{\exp(zF\psi_0/2RT)-1\}\exp(-\kappa x_i)}\right] \quad (25)$$

where κ = Debye-Huckel reciprocal double layer length, which, for aqueous solution at 25 °C, is equal to $3.28\times10^9\sqrt{I}$ m^{-1}.

x_i = radius of a complex molecule adsorbed on the surface. For palladium complex ions, they were surrounded by one hydration sheath, so $x_i = r_i + 2r_w$ (r_w is radius of a water molecule).

$$I = \frac{1}{2}\sum c_i z_i^2$$

z_i = 1 for 1:1 background electrolytes ($NaNO_3$)

The solvation Gibbs Energy, $\Delta G^{o}_{solv,i}$ adjusted by Levine [12] as the difference between the work of charging the ion when situated at a distance R from the interface and that at infinite R, can be written as

$$\Delta G^{o}_{solv,i} = \frac{1}{2} z_i e \Phi_i + \frac{(z_i e)^2}{8\pi\varepsilon_o (r_i + 2r_w)}\left(\frac{1}{\varepsilon_1} - \frac{1}{\varepsilon_b}\right) \quad (26)$$

Φ_i is the potential at a point (r_i+2r_w) in the aqueous phase outside the hydration shell, and is represented as

$$\Phi_i = \frac{z_i e}{8\pi\varepsilon_o\varepsilon_1 x}\left[\frac{f_1+f_2}{|f_1 f_2|^{1/2}}\tan^{-1}|f_1 f_2|^{1/2} - \ln(1+|f_1 f_2|)\right] \quad (27)$$

where

$$f_1 = \frac{\varepsilon_1 - \varepsilon_s}{\varepsilon_1 + \varepsilon_s} \quad (28)$$

$$f_2 = \frac{\varepsilon_1 - \varepsilon_b}{\varepsilon_1 + \varepsilon_b} \quad (29)$$

$$\varepsilon_1 = \left[\frac{\varepsilon_b - 6}{1 + 1.2\times10^{-17}\left(\frac{d\psi}{dx}\right)^2_{x_i}}\right] + 6 \quad (30)$$

where $d\psi/dx$ = dielectric field strength, also obtained from the Gouy-Chapman electric double layer model and evaluated at $x_i = r_w$

$$\frac{d\psi}{dx} = -\frac{2\kappa RT}{zF}\sinh\left(\frac{zF\psi_{x_i}}{2RT}\right) \qquad (31)$$

The chemical component of the free energy, $\Delta G^{\circ}_{chem,i}$ accounts for specific adsorption of some ionic species, regardless of the sign of the surface charge. It is set as a constant, which is adjusted depending on the adsorption behavior.

iii) Liquid Bulk Region (Region III)

The speciation of $PdCl_2$ in the liquid phase when adding NH_4OH into the solution is as follows [13]:

$$PdCl_4^{2-} + NH_3 \leftrightarrow Pd(NH_3)Cl_3^- + Cl^- \qquad K_1 = 3.98\times10^2$$

$$Pd(NH_3)Cl_3^- + NH_3 \leftrightarrow Pd(NH_3)_2Cl_2^0 + Cl^- \qquad K_2 = 5.00\times10^5$$

$$Pd(NH_3)_2Cl_2^0 + NH_3 \leftrightarrow Pd(NH_3)_3Cl^+ + Cl^- \qquad K_3 = 6.33\times10^4$$

$$Pd(NH_3)_3Cl^+ + NH_3 \leftrightarrow Pd(NH_3)_4^{2+} + Cl^- \qquad K_4 = 1.58\times10^4$$

$$NH_3 + H^+ \leftrightarrow NH_4^+ \qquad K_5 = 2.34\times10^9$$

To determine the seven unknowns of complex ion species concentrations at equilibrium, ({$PdCl_4^{2-}$}, {$Pd(NH_3)Cl_3^-$}, {$Pd(NH_3)_2Cl_2^0$}, {$Pd(NH_3)_3Cl^+$}, {$Pd(NH_3)_4^{2+}$}, {NH_4^+}, and {Cl^-}, five speciation equations above and a conservation of mass were solved for 1:1 ratio of NH_4^+:Cl^-.

The multidimensional Newton-Raphson method, which requires a set of initial estimates, was employed to solve the above equations in three regions. The convergence of the Newton-Raphson method is ensured over a wide range of initial estimates. The adsorption model program was written using Matlab®.

Materials and Methods

Oxide Support Preparation

For pure oxide, oxide form of magnesium and copper were prepared by decomposing $Mg(NO_3)_2.6H_2O$ and $Cu(NO_3)_2.3H_2O$ in air at 600°C for 4 h, while alumina (JRC-ALO-6) supplied by Catalysts and Chemicals Ind. Co., Ltd., Japan was used. For composite oxides, they were prepared by a conventional deposition method using nitrate precursors of $Mg(NO_3)_2.6H_2O$ and $Cu(NO_3)_2.3H_2O$. The required amount of metal nitrate precursor was first dissolved in deionized water and the calculated amount of Al_2O_3 was added into the above solution. The slurry was stirred for 24 h and it was slowly boiled and baked in an oven at 110°C for 3 h. The prepared support was then calcined in air at 600°C for 4 h. Two compositions of oxides, 3% and 15% of MgO and CuO on Al_2O_3 were prepared.

Point of Zero Charge and BET Surface Area Measurement

The point of zero charge (pH_{PZC}) of the pure and composite oxides was estimated using a single-point mass titration technique at room temperature, as described in detail by Noh and Schwarz[14]. BET surface area of oxides was obtained using an ASAP 2010 surface area analyzer (Micromeritics Co. Ltd., Norcross, GA, USA). The adsorbate used in the adsorption method for area determination was nitrogen.

Experimental Adsorption of Pd on Pure and Composite Oxides

Pd was loaded on the prepared support by dissolving the calculated amount of $PdCl_2$ in an excess of HCl with the molar HCl to $PdCl_2$ ratio of 5.6:1. The initial

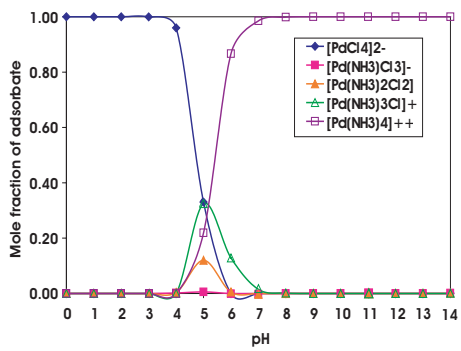

Fig 2. The pH dependence of equilibrium mole fraction of Pd species

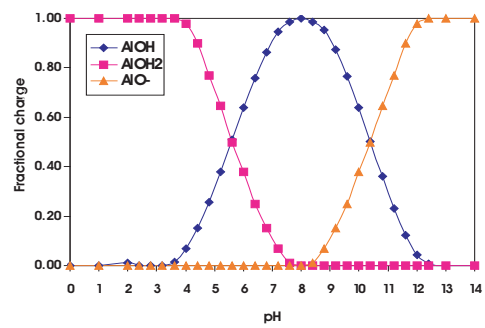

Fig 3. Surface charge speciation as a function of pH on Al_2O_3

concentration of palladium in the impregnated solution was prepared to provide a monolayer of palladium chloride complex surrounded by one hydration sheath[15]. It was 2.71 x 10^{-3} M for alumina and 1.694 x 10^{-4} M for both MgO and CuO. Since the initial palladium solution had a pH value around 1.96, the initial pH values studied (3-11) were obtained and maintained by adding NH_4OH and HCl before adding the support. In these experiments, the ionic strength, which is

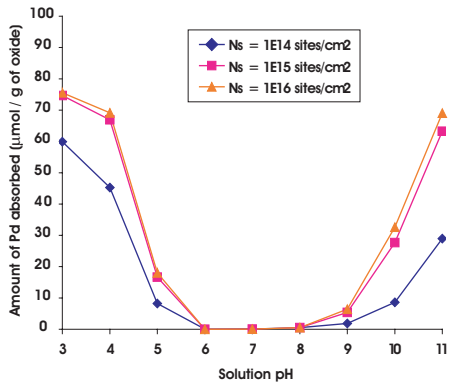

Fig 4. Effect of number of surface sites on Pd adsorption on Al_2O_3

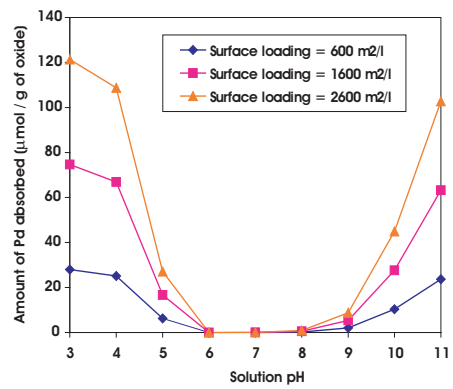

Fig 5. Effect of surface loading on Pd adsorption on Al_2O_3

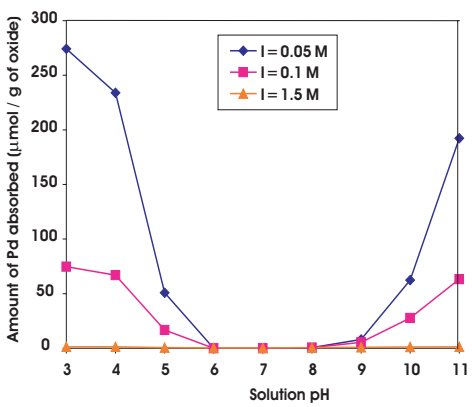

Fig 6. The effect of ionic strength on Pd adsorption on Al_2O_3

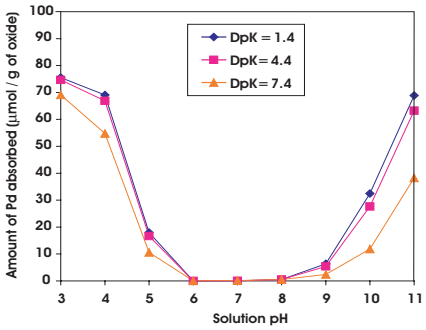

Fig 7. Effect of the difference in the two pK^{int} values on Pd adsorption on Al_2O_3

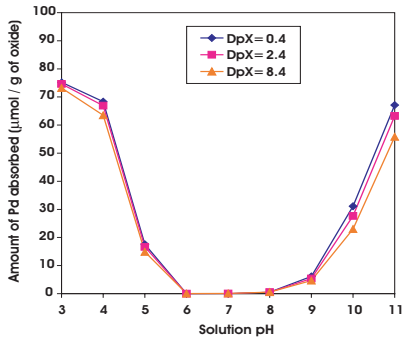

Fig 8. Effect of the difference between the intrinsic equilibrium constants of background electrolyte on Pd adsorption on Al_2O_3

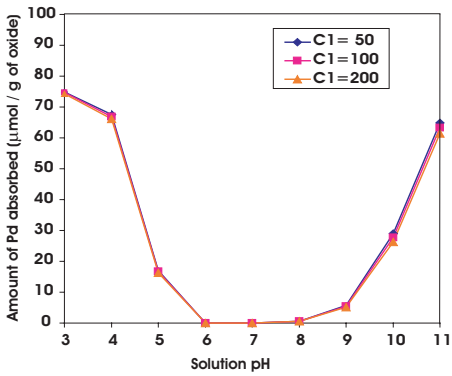

Fig 9. Effect of inner layer capacitance(C_1) on Pd adsorption on Al_2O_3

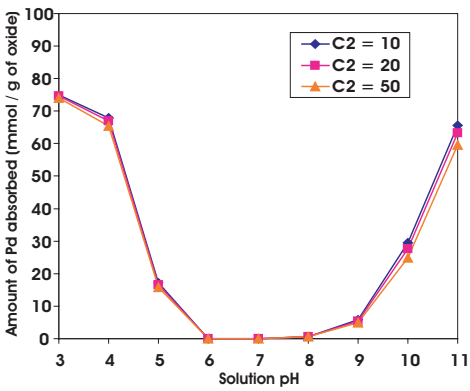

Fig 10. Effect of outer layer capacitance(C2) on Pd adsorption on Al_2O_3

determined from the amount of ions in the impregnated solution, was controlled by adding $NaNO_3$ as background electrolyte into the above solution. The surface loadings of Al_2O_3, MgO and CuO in solution were controlled at different values, 1600, 100, and 100 m^2/l, respectively, since Al_2O_3 having a much higher surface area than MgO and CuO.

Adsorption of palladium on composite oxides was conducted in a similar manner as that of pure oxides. The surface loading of composite oxides was set at 1600 m^2/l. These slurries were then stirred and mixed on an orbital shaker at 200 rpm for 24 h. The final pH or the equilibrium pH was measured and would be used as a parameter in the model. Thereafter, the suspended solution was vacuum filtered through a membrane disc. Liquid solution after filtration was further analyzed by atomic absorption spectroscopy (AA 457 of Instrumentation Laboratory Inc.) to obtain the final palladium concentration. The amount of Pd adsorbed on the oxide was calculated by the difference between the initial and final Pd concentrations.

Results and Discussion

Point of Zero Charge and BET Surface Area of Oxides

The pH at point of zero charge and BET surface area of the oxides obtained from mass titration is shown in Table 1. The points of zero charge of Al_2O_3, CuO, and MgO were about 8.0, 6.5, and 12.0, respectively. This indicates that at pH 12.0 both negatively charged and positively charged sites on the MgO surface are in balance, while for Al_2O_3 and CuO both charge types are balanced at pH close to 7.0. These estimated points of zero charge show the high anionic property of MgO and amphoteric properties of Al_2O_3 and CuO. Considering the pH_{PZC} of the composite oxides, their values are in between that of two pure supports. Similar to the pH_{PZC} results, BET surface areas of composite oxides lie in between that of pure oxides. When the contents of MgO and CuO increase, the BET surface areas of the composite oxides are decreased because the surface areas of MgO and CuO are lower than that of Al_2O_3.

Table 1 The pH at the point of zero charge and BET surface area of oxides

Oxide	pH at the point of zero charge (pH_{PZC})	BETSurface Area (m^2/g)
Al_2O_3	8.0	188.9
$3\%MgO/Al_2O_3$	8.58	160.4
$15\%MgO/Al_2O_3$	10.8	131.0
MgO	12.0	3.7
$3\%CuO/Al_2O_3$	7.85	165.5
$15\%CuO/Al_2O_3$	6.94	142.3
CuO	6.48	3.9

Experimental Determination and Modeling of Pd Adsorption on Pure Oxides

The amount of adsorption of Pd complex ion from aqueous solution onto an oxide surface depends largely on the charge of both surface oxide and palladium complex ions. Palladium complex ion forms are changed due to the pH of the solution. By controlling pH with the known values of equilibrium constants, palladium speciation change with pH is calculated as illustrated in Fig 2. For speciation of a solid oxide surface, knowing the pH_{PZC}, the charge on a solid oxide surface could be determined from eqs. (3), (4) and (18), as shown in Fig 3 for Al_2O_3. Similar speciation behavior was also obtained with MgO and CuO with different fractional types of species.

Sensitivity Analysis of Adsorption Parameter Values

In simulation of the adsorption of Pd on oxides, the sensitivity analysis, which examines how sensitive the model results are to the model parameters chosen to estimate their values was first performed. Pd adsorption on Al_2O_3 in the pH range of 3-11 was the system to be studied. Five adjustable model parameters, total number of surface sites (N_s), intrinsic equilibrium constants for proton adsorption and desorption in terms of DpK, intrinsic equilibrium constants of the background electrolyte in terms of DpX and integral capacitances in the electrical double layer (C_1 and C_2), and two experimental parameters, ionic strength (I) and surface loading were considered. The simulation results are illustrated in Figs 4-10.

In the common ranges of parameter values studied[9,16], three tendencies of the influence of parameters on Pd adsorption can be categorized. The first one is the group of parameters that enhance the Pd adsorption. These parameters are N_s and surface

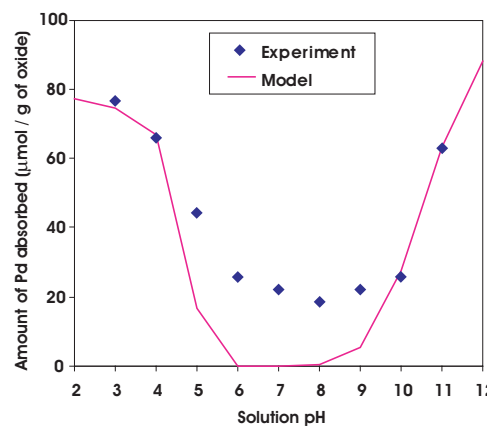

Fig 11. Variation of amount of Pd adsorbed (µmol/g of oxide) as a function of solution pH with initial concentration of $2.71x10^{-3}$ mol/l at 1600 m^2/l surface loading of Al_2O_3

loading, which obviously represent the amount of active sites ([SOH_2^+], [SOH], [SO^-], [SOX^+], and [SOY^-]) and surface area of oxide available in the solution. As N_s and surface loading are increased the adsorption is increased as seen in Figs 4 and 5. Nevertheless, there was a small discrepancy in the adsorption results between these two parameters. For the surface loading effect, the simulation results show that the higher the surface loading value, the higher the amount of Pd adsorbed. On the other hand, the amount of Pd adsorbed was initially increased as the number of active sites (N_s) was increased from 1×10^{14} to 1×10^{15} sites/cm^2, but beyond this value the amount of Pd adsorbed changed little, although the N_s was increased by one order of magnitude.

The second group of parameters, i.e., ionic strength, DpK and DpX, inhibits the Pd adsorption as these parameters are increased. The simulation results of the effect of ionic strength, DpK and DpX are presented in Figs 6-8. If the ionic strength that was normally a fixed amount of 1:1 background electrolyte in the adsorption system was increased at each pH value by adding more electrolyte, the electrical double layer around the oxide particle was compressed. The amount of Pd adsorbed on oxide would be decreased. Considering DpK and DpX, DpK is related to the intrinsic equilibrium constants of surface and the point of zero charge of the oxide, while DpX is the difference between the intrinsic equilibrium constants of cations and anions in the background electrolytes. With the decrease of DpK and DpX the adsorption is decreased. The last group of parameters shows very little influence of their variations on Pd adsorption for the entire pH range, as illustrated in Figs 9 and 10.

These sensitivity analysis results of the model were not far from what was expected theoretically. Therefore it was considerably qualified to be used to further simulate and predict the Pd adsorption on other pure oxides and composite oxides.

The model's parameters used in the adsorption model for Pd adsorption on pure oxides were estimated as discussed previously. For example, the DpK and DpX values of an oxide was first chosen, and pK_{a1}^{int}, pK_{a2}^{int}, pK_x^{int} and pK_y^{int} were then adjusted until the best match was obtained. N_S of CuO and MgO were estimated based on their BET surface areas. The values are concluded in Table 2 and 3 for Region I, and Region II and III, respectively.

Table 3 Model's parameters for pure oxides (Region II and Region III)

Oxide	ε_s	Surface loading (m^2/l)	ΔG_{chem} (kJ/mol)	Ionic strength (mol/l)
Al_2O_3	12.30	1600	0	0.1
MgO	3.20	100	-19.00	1.5
CuO	9.77	100	-19.00	1.5

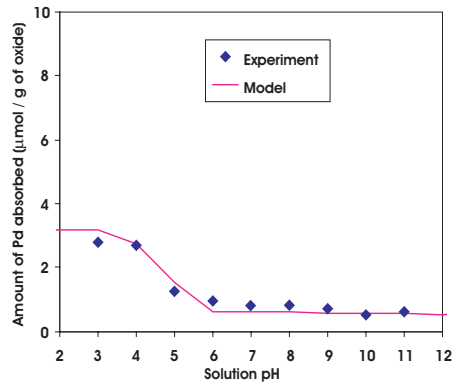

Fig 12. Variation of amount of Pd adsorbed (µmol/g of oxide) as a function of solution pH with initial concentration of 1.694×10^{-4} mol/l at 100 m^2/l surface loading of MgO from the experiment and the adsorption model

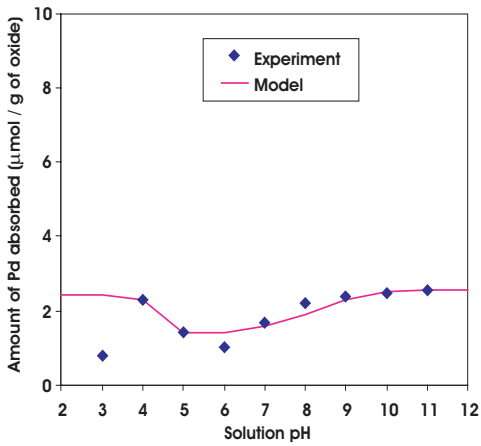

Fig 13. Variation of amount of Pd adsorbed (µmol/g of oxide) as a function of solution pH with initial Pd concentration of 1.694×10^{-4} mol/l at 100 m^2/l surface loading of CuO from the experiment and adsorption model

Table 2 Model's parameters for Pd adsorption on pure oxides (Region I)

Oxide	DpK	pK_{a1}^{int}	pK_{a2}^{int}	DpX	pK_x^{int}	pK_y^{int}	N_s(site/cm^2)	C_1(µF/cm^2)	C_2(µF/cm^2)
Al_2O_3	4.40	5.80	10.20	2.40	9.20	6.80	1.0×10^{15}	100	20
MgO	4.00	10.00	14.00	7.10	14.00	6.90	1.9×10^{13}	100	20
CuO	3.96	4.50	8.46	3.80	8.50	4.70	2.0×10^{13}	100	20

Adsorption of Pd on Al_2O_3

The experimental and the calculated amount of Pd adsorbed on Al_2O_3 varied with the equilibrium solution pH, as compared in Fig 11. At pH below the pH_{PZC} of Al_2O_3, 3 - 7, the amount of Pd adsorbed increased when pH decreased. This can be explained by considering that the surface charge of oxides and the palladium complex ion forms varied with pH in Figs 2 and 3. At low pH, alumina surface tended to be more positively charged, so a high amount of Pd complex anions ($PdCl_4^{2-}$) can be adsorbed on this positively charged surface. When the pH was more than 8 (above pH_{PZC}), the negatively charged surfaces increased drastically, while the positively charged surface disappeared. In this pH range, Pd complex cations, $Pd(NH_3)_4^{2+}$, would be adsorbed on this negative surface and this resulted in high Pd adsorption when pH increased. Weak adsorption was observed at pH around 8, since the solid surface had the same electrical potential as that of the bulk of the contacting solution. Hence, the overall charge of the particle was zero (neutral surface zone).

In the comparison between the experiment and the mathematical model, the trend of Pd adsorption was similar, but they were different in terms of magnitude. In the pH range of 3 - 5 and 9 - 11, the agreement was reasonably good. For the pH range of 6 - 8, however, the predicted results were relatively low compared to the experimental results. In practice, when the oxide was maintained near the range of pH_{PZC} although its net charge was zero, there exists some inventory of positive, negative, and neutral surface groups[17]. Hence, small amount of Pd can be adsorbed on surface. On the other hand, the mathematical model considered the overall net charge on alumina surface was zero at this point, so there was no adsorption of Pd on the surface [13].

Adsorption of Pd on MgO

The adsorption of Pd on MgO is shown in Fig 12. The amount of Pd adsorbed on MgO decreased when the solution pH increased from 3 to 11. The maximum and minimum Pd adsorption occurred at solution pH of 3 and 11 (close to the pH_{PZC} of MgO), respectively. From pH 3 to 11 the surface of MgO is significantly positively polarized, which makes possible for its surface to adsorb Pd complex anions (mainly $PdCl_4^{2-}$) formed in solution in the pH range of 3 - 4. Above pH 3, Pd complex anions ($PdCl_4^{2-}$) decreased, which resulted in diminishing Pd adsorption, and when the pH was more than 8, the charge of Pd complex ions in the solution was positive ($Pd(NH_3)_4^{2+}$), while the surface charge of MgO was close to neutral. Hence, there was little Pd adsorption on the surface of MgO when the solution pH was higher than 8.

Adsorption of Pd on CuO

The result of Pd adsorption on CuO at different solution pH (3-11) is shown in Fig 13. When the pH was lower than 6, the amount of Pd (mostly $PdCl_4^{2-}$) adsorbed on the positively charged surface increased with decreasing pH, except at pH 3. Since CuO is an amphoteric oxide, there are two types of oxide charge: either an anionic precursor solution with a pH lower than 6, or a cationic precursor solution with a pH higher than 6. The adsorption was minimum at pH 3, not pH_{PZC}, because it was observed from the experiment that CuO was agglomerated and settled out from the solution. Similar to Pd adsorption on Al_2O_3, when the pH was higher than pH_{PZC}, the adsorption of Pd on the negatively charged surface increased.

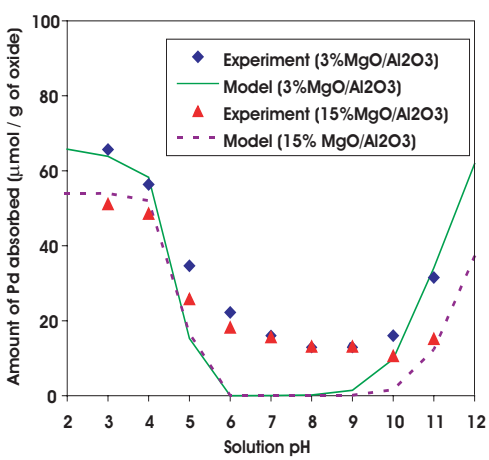

Fig 14. The comparison of the amount of Pd adsorbed on 3%, and 15 % MgO/Al_2O_3 (mmol / g of oxide) between experiment and adsorption model

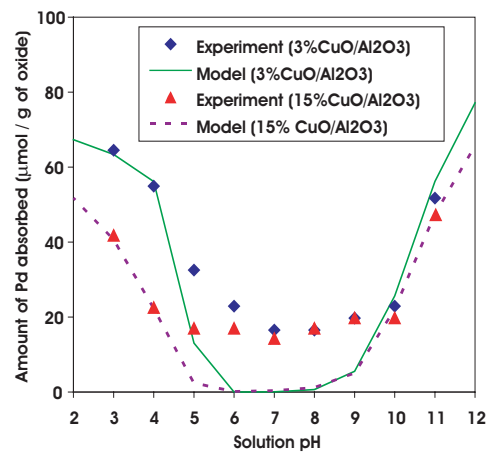

Fig 15. The comparison of the amount of Pd adsorbed on 3%, and 15 % CuO/Al_2O_3 (mmol/g of oxide) between experiment and adsorption model

Experimental and Modeling of Pd Adsorption over Composite Oxides

The model's parameters for Pd adsorption on composite oxide in the model mostly were determined from that of pure oxides and some of them were the same as that of pure oxides. The values are presented in Tables 4 and 5. The chemical Gibbs Free Energy, ΔG_{chem}, representing the specific adsorption phenomenon in the adsorption model for all cases was taken as zero (both composite oxides and both concentrations of promoter) to best match most of the experimental data. The effects of pH, and type and concentration of promoter on the Pd adsorption over composite oxide is discussed below.

Adsorption of Pd on 3% and 15% MgO/Al_2O_3

From Fig 14, for 3% MgO/Al_2O_3, the trend for experimental adsorption of Pd onto the oxide was similar to the case of Pd adsorption onto pure Al_2O_3. The amount of Pd adsorbed increased at pH below and above 7-8, which is the pH_{PZC} of this composite oxide, and minimum adsorption occurred close to pH_{PZC} of pure alumina. This is because Al_2O_3 was the dominant species in this composite oxide. When the amount of MgO was increased to 15%, the shape of the adsorption curves from both the experiment and the model was similar to that of 3% MgO/Al_2O_3, but with lower magnitude. From the experimental results, higher amounts of Pd were adsorbed at pH lower and higher than the pH_{PZC} of MgO/Al_2O_3. This experimental adsorption trend is more influenced by the amount of MgO, especially at pH near the pH_{PZC} of MgO. In other words, when more MgO was added, the shape of Pd adsorption on MgO/Al_2O_3 was close to that of MgO. The predicted adsorption capacity from the model agreed well with the results from the experiment in the pH range above and below pH of 6-10 (range of pH_{PZC}).

Adsorption of Pd on 3% and 15% CuO/Al_2O_3

From Fig 15, the trends of Pd adsorption over 3% CuO/Al_2O_3 and 15% CuO/Al_2O_3 from both the experiment and model were similar to those of pure Al_2O_3. At both concentrations of CuO, the amount of Pd adsorbed was high over the pH ranges of 3 - 6 and 10 - 11. The minimum Pd adsorption occurred at pH ~ 6 - 8, which is near the pH_{PZC} of CuO/Al_2O_3. The adsorption capacity of 15% CuO/Al_2O_3 was the lowest comparing with that of pure Al_2O_3 and 3% CuO/Al_2O_3. However, in the pH range near pH_{PZC} (6 - 9), the %CuO had no effect on the adsorption capacity, which corresponded with the results predicted by the model.

At pH lower than the pH_{PZC} of the composite oxide, it was found that for adsorption on composite oxides, palladium complex ions selectively adsorb on Al_2O_3 more than on MgO and CuO, due to the higher surface area of Al_2O_3. However, at pH higher than the pH_{PZC} of the composite oxide, palladium complex ions selectively adsorbed and adsorption capacity was strongly affected by the CuO and MgO promoter. This influence was obviously observed at high percentage of promoter. Overall, the promoter concentration induced the adsorption of Pd in such a way that, when the concentration of promoter increased, the amount of Pd adsorbed decreased. This is because the amount of Al_2O_3, which provides high surface area, was decreased.

Comparison of Pd Adsorption between 3% MgO/Al_2O_3 and 3% CuO/Al_2O_3

The effect of nature of promoter on support (3% MgO/Al_2O_3 and 3% CuO/Al_2O_3) is shown in Figs14 and 15. The trends of the results were similar to the case of 15% MgO/Al_2O_3 and 15% CuO/Al_2O_3. When the pH is lower than 6, 15% MgO/Al_2O_3, which has low surface area compared to 15% CuO/Al_2O_3, can adsorb more Pd than 15% CuO/Al_2O_3. It also confirms that Pd adsorption was dependent on the type of promoter. The type of promoter would generally indicate the charge at the oxide surface (positively charged or negatively charged surface site). The oxide surface tended to polarize positively and to adsorb compensating anions, when the solution pH was lower than pH_{PZC}. On the contrary, the oxide in a solution at a pH higher than the pH_{PZC} would have an excess amount

Table 5 Model's parameters for pure oxides (Region II and Region III)

Oxide	ε_s	Surface loading (m^2/l)	ΔG_{chem} (kJ/mol)	Ionic strength (mol/l)
3%MgO/Al_2O_3	10.44	1600	0	0.1
15%MgO/Al_2O_3	8.53	1600	0	0.1
3%CuO/Al_2O_3	10.77	1600	0	0.1
15%CuO/Al_2O_3	9.27	1600	0	0.1

Table 4 Model's parameters for composite oxides (Region I)

Oxide on Al_2O_3	DpK	pK_{a1}^{int}	pK_{a2}^{int}	DpX	pK_x^{int}	pK_y^{int}	Ns(site/cm^2)	C_1(mF/cm^2)	C_2(mF/cm^2)
3%MgO	5.28	5.94	11.22	2.40	9.20	6.80	0.849×10^{15}	100	20
15%MgO	6.00	7.80	13.80	2.00	7.00	5.00	0.690×10^{15}	100	20
3%CuO	4.70	5.50	10.20	2.40	9.20	6.80	0.876×10^{15}	100	20
15%CuO	6.50	3.69	10.19	4.00	9.50	5.50	0.753×10^{15}	100	20

of negatively charged surface due to the charge compensation by the adsorbed cations.

Comparison of Pd Adsorption between15% MgO/Al_2O_3 and 15% CuO/Al_2O_3

From the previous section, it was found that BET surface area of 15%CuO/Al_2O_3 was higher than that of 15%MgO/Al_2O_3 (142.3 and 131.0 m^2/g, respectively). Hence, it should adsorb much more Pd on the surface. But when the pH was lower than 6, 15% MgO/Al_2O_3 adsorbed more Pd than 15% CuO/Al_2O_3. This means that the surface area of the catalyst was not the only factor that affects the adsorption phenomena, there were other factors, such as the nature of the support, which depends on the type of promoter. The type of promoter would determine the oxide properties such as the point of zero charge (pH shift of 15% MgO/Al_2O_3 from Al_2O_3 is ~+2.8 while it was ~ -1.0 for 15% CuO/Al_2O_3). Therefore, different types of promoter having different points of zero charge and shapes of zeta potential of the oxide can influence the Pd adsorption.

Conclusions

Composite oxide properties are generally in between the two pure oxides. An amphoteric oxide promoter, CuO, showed similar adsorption behavior to the main oxide component, Al_2O_3, while a basic oxide promoter, MgO showed different behavior. As promoter increased, Pd adsorbed selectively more on its surface. However, since both MgO and CuO promoters have lower surface area than Al_2O_3, the adsorption capacities of the composite oxides were less than Al_2O_3. The triple layer adsorption model used in this work can predict the adsorption/wet impregnation of Pd complex ions on both composite oxides well over most of the pH range of 3-11, except the pH range near pH_{PZC}. The suggested pH value for preparing $Pd/MgO/Al_2O_3$ and $Pd/CuO/Al_2O_3$ composite oxides is the pH close to the initial pH of the palladium precursor solution.

Notation

C_1	Inner layer capacitance in an electrical double layer
C_2	Outer layer capacitance in an electrical double layer
C_i	The bulk concentration of the ion in the solution (mol/m^3)
e	Charge of electron (elementary charge), 1.6×10^{-19} C
F	Faraday's constant, 96485 C/mol or 6.02×10^{23} e
$\Delta G^o_{ads,i}$	Gibbs free energy of adsorption
$\Delta G^o_{chem,i}$	Gibbs free energy of chemical
$\Delta G^o_{coul,i}$	Gibbs free energy of coulombic
$\Delta G^o_{solv,i}$	Gibbs free energy of solvation
I	Ionic strength (mol/l)
k	Boltzmann constant, 1.38×10^{-23} J/K
$K^{int}_{a_1}$	Intrinsic ionization constant of adsorption of proton reaction
$K^{int}_{a_2}$	Intrinsic ionization constant of desorption of proton reaction
K^{int}_{x}	Intrinsic ionization constant of background electrolyte (cation)
K^{int}_{y}	Intrinsic ionization constant of background electrolyte (anion)
N_A	Avogadro's number , 6.02×10^{23} molecules/mol
N_S	Total number of site available, sites/cm^2
P	The operational pressure
R	Gas constant , 8.314 J/gmol K
r_i	Radius of adsorbate species (m)
$r_{hydrated}$	Radius of hydrated ion (m)
r_w	Radius of water molecule (1.38×10^{-10} m)
T	Absolute temperature, K
$\{X^+\}$	Concentration of cationic species in bulk phase
$\{Y^-\}$	Concentration of anionic species in bulk phase
z	Valence of ion
Γ_i	Adsorption density (mol/m^2)
$d\psi/dx$	Dielectric field strength
ε_b	Relative dielectric constant of the medium = 78.5 for water
ε_s	Relative dielectric constant of the solid oxide
σ_o	Surface charge density, $\mu C/cm^2$
σ_β	Charge density at β plane
σ_d	Charge density at diffuse layer plane
κ	Debye-Huckel reciprocal double layer length
ψ_d	Potential at diffuse layer plane
$\psi_{x,i}$	Solution of the Laplace 's equation subject to the surface
ψ_o	Surface potential and bulk boundary condition of aqueous solutions at 25°C
[ ]	Surface concentration, mol/l
{ }	Solution or bulk concentration, mol/l
PZC	Point of zero charge of the oxide
pH_{PZC}	pH at the point of zero charge
S, s	Surface

REFERENCES

1. Yates, D.E., Levine, S., and Healy, T.W. (1974) Site binding model of the electrical double layer at the oxide/water interface. *J. Chem. Soc. Faraday Trans. I* **70**, 1807-18.
2. Davis, J.A., James, R.O., and Leckie, J.O. (1978) Surface Ionization and Complexation at the Oxide/Water Interface. *J. Colloid Interface Sci.*, **63**, 480-99.
3. James, R.O., Davis, J.A., and Leckie, J.O. (1978) Computer simulation of the conductometric and potentiometric titrations of the surface groups on ionizable latexes. *J. Colloid Interface Sci.*, **65**, 331-44.
4. Westall, J. and Hohl, H. (1980) A comparison of electrostatic models for the oxide/solution interface. *Adv. Colloid Interface Sci.*, **12**, 265-94.
5. Wood, R., Fornasiero, D. and Rarlston, J. (1990) Electrochemistry of the boehmite-water interface. *Colloids and Surfaces*, **51**, 389-403.
6. Robertson, A.P. and Leckie, J.O. (1997) Cation binding predictions of surface complexation models: Effect of pH, ionic strength, cation loading, surface complex, and model fit, *J. Colloid Interface Science*, **188**, 444-72.
7. Tien, C. (1994) Representation, correlation, and prediction of single-component adsorption equilibrium data. In : *Adsorption Calculations and Modeling*, pp.15-41. Butterworth-Heinemann, New York.
8. Tewari P.H. (1981) Surface chemistry and adsorption properties of milled chrysotile asbestos fibres. *Adsorption from Aqueous Solutions*, pp. 220-39. Plenum Press, New York.
9. Schwarz, J.A., Ugbor, C.T. and Zhang, R. (1992) The adsorption impregnation of Pd(II) cations on alumina, silica, and their composite oxides. *J. Catalysis*, **138**, 38-54.
10. James, R.O. and Healy, T.W. (1972) Adsorption of hydrolyzable metal ions at the oxide-water interface I. Co (II): Adsorption on SiO_2 and TiO_2 as model system. *J. Colloid Interface Sci.*, **40**, 42-52.
11. James, R.O. and Healy, T.W. (1972) Adsorption of hydrolyzable metal ions at the oxide-water interface III. A thermodynamic model of adsorption. *J. Colloid Interface Sci.*, **40**, 65-81.
12. Levine, S. General Discussion. *Faraday Soc.*, **52**, 320-23.
13. Contescu, Cr. and Vass, M.I. (1987) The effect of pH on the adsorption of palladium (II) complexes on alumina. *Appl. Catal.*, **33**, 259-71.
14. Noh, J.S., and Schwarz, J.A. (1989) Estimation of the point of zero charge of simple oxides by mass titration. *J. Colloid Interface Sci.*, **130** (1), 157-64.
15. Santhanam, N.K., Conforti, T., Spieker, W. and Regalbuto, J.R. (1994) Nature of metal catalyst precursors adsorbed onto oxide supports. *Catal. Today*, **21**, 141-56.
16. Lutzenkirchen, J. (1998) Parameter estimation for the triple layer model. Analysis of conventional methods and suggestion of alternative possibilities, *J. Colloid Interface Sci.*, **204**, 119-27.
17. Brunelle, J.P.(1978) Preparation of catalysts by metallic complex adsorption on mineral oxides, *Pure & Appl.Chem.*, **50**, 1211-29.